Journal of
Composites Science

MDPI

Article

Increasing the Efficiency of Multilayered Silicate Melt Incorporation into Starch-Based Polymeric Matrices

Doina Dimonie [1,2], Ramona Marina Grigorescu [1], Bogdan Trică [1,*], Celina-Maria Damian [2], Eugeniu Vasile [2], Roxana Trusca [2], Cristian-Andi Nicolae [1], Diana Constantinescu-Aruxandei [1] and Florin Oancea [1,*]

[1] Polymers and Bioresources Departments, National Institute for Research and Development in Chemistry and Petrochemistry-ICECHIM, Splaiul Independentei nr. 202, Sector 6, 060021 Bucharest, Romania; ddimonie@yahoo.com (D.D.); ramona.grigorescu@icechim.ro (R.M.G.); diana.constantinescu@icechim.ro (D.C.-A.)
[2] Chemical Engineering and Biotechnologies Faculty, National University of Science and Technology Politehnica Bucharest, Splaiul Independentei 313, Sector 6, 060042 Bucharest, Romania; celina.damian@upb.ro (C.-M.D.); eugeniu.vasile@upb.ro (E.V.); roxana_doina.trusca@upb.ro (R.T.)
* Correspondence: bogdan.trica@icechim.ro (B.T.); florin.oancea@icechim.ro (F.O.)

Abstract: This article compares two exfoliation options of multilayered silicate, one considering the action of shear stress and temperature during melt compounding and another taking into account the action of the thermo-mechanical pretreatment of multilayered silicate in a plasticizer common to the starch and polyvinyl alcohol (PVOH), the two polymers from the compound. Increasing the action time of the shear stress and temperature during melt compounding proved to be an ineffective method for silicate exfoliation following the high degradability of starch and PVOH under thermo-mechanical conditions and the loss of hydration of the multilayered silicate under thermo-mechanical conditions. The obtained results prove that, by pretreating before embedding into the desired starch-PVOH matrix, it was possible to cancel the electrostatic attractions between the component lamellae of a multilayered silicate. During melt compounding with the two polymers, new attractions between the obtained lamellae and the polar groups of each polymer from the blend were settled, and so, without the usage of a liquid plasticizer, exfoliated intercalated nanocomposites were achieved. The improved properties and the practical importance of the new nanocomposites regards the obtaining of a non-degradable material that has a white color, better elastic properties and thermal stability, and a higher dissipation capacity of deformation energy.

Keywords: multilayered silicate; delamination; pretreatment; melt compounding; exfoliated-intercalated nanocomposites; starch

Citation: Dimonie, D.; Grigorescu, R.M.; Trică, B.; Damian, C.-M.; Vasile, E.; Trusca, R.; Nicolae, C.-A.; Constantinescu-Aruxandei, D.; Oancea, F. Increasing the Efficiency of Multilayered Silicate Melt Incorporation into Starch-Based Polymeric Matrices. *J. Compos. Sci.* **2024**, *8*, 72. https://doi.org/10.3390/jcs8020072

Academic Editor: Francesco Tornabene

Received: 2 December 2023
Revised: 14 January 2024
Accepted: 7 February 2024
Published: 11 February 2024

1. Introduction

As it is well known, polymer nanocomposites are a class of composites containing inorganic nanoparticles dispersed in an organic polymer matrix to improve the performance of the matrices [1–4]. Due to the limitation of conventional polymer resources, in view of preparing sustainable alternatives for tomorrow, the 2050 perspective of polymer materials mainly considers matrices based on polymers of renewable origin and those achieved via recycling of post-consumer goods [5–9]. The compounds focused on polymers of renewable origin can be a viable and sustainable alternative only with the condition of controlling their functional properties and increasing their durability. This is in agreement with the requirements of applications, such that the nanocomposites with these matrices can be of practical interest [7,8,10–14]. The most common polymer blends are those of an immiscible nature that differ from the miscible ones through the interface nature of the interactions between the macromolecules. These interactions, in turn, depend on the chemical structure of the phases in contact, ultimately controlling the functional properties and the applications

of the new compounds [15–19]. Nanocomposites with layered silicates are types of compounds in which the macromolecules are arranged between the silicate platelets or between the individual lamellae to generate stable compounds with thermo-mechanical properties of practical interest (e.g., Young's modulus, storage modulus, thermal stability, etc.) at low silicate concentrations [20–23]. The methods of obtaining polymer nanocomposites with the widest practical applicability are in solution, in situ intercalative polymerization, and intercalation during melt compounding [2,6–9,22]. The main parameters that control the nature and properties of polymeric nanocomposites with layered silicate content are the type of polymer and silicate, the method of treating the silicate galleries, the incorporation method of the silicate into the polymer matrix, and the efficiency of the exfoliation methods on multilayered silicates. The effectiveness of multilayered silicate exfoliation depends on the targeted technique of obtaining the desired nanocomposites. If these techniques relate to solution methods, the problems are simplified, contrasting with silicate embedding using melt compounding when customized solutions for each group of polymer matrices are needed [2,19–23]. Melting techniques for obtaining new nanocomposites are of interest for products with special shapes that are required in large quantities on the market. Among the nanocomposites with matrices based on renewable polymers, there are those containing starch [24–26], but the general conclusion about the limitations in their development is related to the dispersion difficulties of the nanofiller into the matrix. Regarding the nanocomposites based on starch, polyvinyl alcohol, and layered silicate, several studies were carried out to identify the dependence of the morphology and thermal properties on the type of layered silicate to find the most efficient functional group with which the silicate galleries can be treated [27–36]. Other studies have focused on the silicate incorporation method into the polymer blends [37], the target filling content [38–42], the dependence of the degree of miscibility on the type of components of the layered silicate mixtures, or the influence of the miscibility degree on the surface defects [43–45]. It was observed that the intercalation degree into a starch-PVOH matrix increased if natural multilayered silicate (NaMMT) or NaMMT functionalized with small-volume ammonium ions (Nanocor I 28) were used. Nanostructured or micro-structured composites can be obtained using this approach [35,36,38–42]. The incorporation of NaMMT into such matrices during melt compounding without any other treatment [38–42] or by subjecting the layered silicate to a minor mechanical treatment before incorporation into the melts [37,46] was previously studied, but the results were not optimal. That is why finding a more effective dispersion method for the melt compounding of layered silicates into a starch-PVOH matrix is of both scientific and practical relevance. The scientific interest is related to the finding of a method to diminish or eliminate the rejection forces between the multilayers of the silicate so that to achieve suitable dispersion into a polymeric polar matrix, and the practical one is to create new nanocomposites based on starch with improved properties without using another liquid plasticizer.

To achieve new nanocomposites based on starch with controlled morphologies, this article presents the exfoliation challenge via two methods, the efficiency of which is compared: one with the help of shear stress and temperature during melt compounding and the second one by applying a thermos-mechanical treatment before melt compounding with starch and PVOH.

2. Materials and Methods

2.1. Materials

The following materials were used: native corn starch, with 13.1% moisture, 2.2% acidity, and pH 4.9, which melts at 263 °C and has a crystalline phase content of 30.6%; polyvinyl alcohol with a maximum degree of hydrolysis (85 mol%), residual polyacetate content of 15 mol%, viscosity of 27–33 cP, and specific heat of 1674 J/kg K. The PVOH used has a glass transition at 83 °C and melts at 258 °C. The melting process is reversible upon cooling when crystallization occurs. The crystalline phase content of PVOH is 33%; montmorillonite (MMT): M_x ($Al4_{yx}$ Mg_x) and $8O_{20}(OH)_4$ has no treated galleries; alkyl

quaternary ammonium-modified montmorillonite (Nanocor I28); plasticizers for both starch and PVOH: water.

2.2. Procedure

The delamination of multilayered silicate can be facilitated either via shearing stress and temperature during melt compounding or via mechanical stress and temperature acting over a liquid into which the silicate is placed. This liquid can be selected to interact with both the silicate and the polymers and, at the same time, to be a common plasticizer for the polymers from the blend into which the silicate is incorporated.

For the multilayered silicate delamination, the following two procedures were compared, at first sight, they are extremely accessible and easily performed, namely through:

1. The delamination of the silicate by following the next three successive steps: (a) embedding the silicate into the polymer matrix, (b) the analysis of both the silicate's thermal behavior and its morphology before and after delamination in Brabenderplasticorder, (c) measuring the color of the nanocomposites containing the delaminated silicate. Thus, Nanocor I28 (a functionalized multilayered silicate compound with small-volume ammonium ions) was delaminated into a thermo-mechanical environment by controlling the time, temperature, and shear stress in a laboratory Brabender plastograph for 90 min at 75 rpm and two different temperatures, 140 °C and 200 °C, followed by X-ray diffraction (XRD) characterization and comparing the obtained morphologies after 90 min to the initial one. In addition, the silicate compound was thermally characterized by recording the thermograms in dynamic (differential scanning calorimetry (DSC), thermogravimetric analysis (TGA)) and isothermic conditions (140 °C and 200 °C). For step (a), a blend with 70% starch, 30% PVOH, and 4% multilayer silicate was compounded in a Brabender plasticorderat 120 °C for 30 min at 75 rpm, and the obtained compounds were rolled into a sheet using a laboratory roller. The color of the resulting sheets was measured according to Section 2.3;
2. The thermo-mechanical treatment of NaMMT in a controlled process before incorporation into the polymer matrix by placing the multilayered silicate in an effective plasticizer for both the polymers, i.e., starch and polyvinyl alcohol, stirring the system, which is heated to a certain temperature. The periodic sampling of such treated multilayered silicate mixture and the incorporation of the thermo-mechanically pretreated silicate via melt compounding into the same matrix of starch modified with PVOH with the same formulation and conditions as procedure 1, was done. The selected plasticizer was water, and the sampling times varied up to 288 h as follows: 8, 16, 24, 72, and 288 h. The system consisted of NaMMT and water and which was stirred in a laboratory shaker at 50 °C and 100 rpm. Periodically, the samples of the treated silicate were taken and embedded in the same polymeric matrix (formulation: 4% thermo-mechanically treated silicate with 70% starch and 30% PVOH) and under the same conditions (120 °C, 75 rpm, and 5 min homogenization after melting). The morphologies of the obtained composites were analyzed according to Section 2.3. The resulting compounds were shaped as sheets using a laboratory roller operated at 85 °C, with roller cylinder speeds of 24 rpm/28 rpm. The silicates used were selected such that each of them to represent the most difficult option for each chosen studying delamination solution. Due to the functional group content, the silicate with treated galleries, Nanocor I28 could have poor stability in the thermo-mechanical conditions due to the Brabender plasticorder, and, therefore, it was checked. Because the NaMMT has narrower galleries than a functionalized version, Nanocor I 28, its interaction with water can be more difficult to be done and, therefore, it was studied.

2.3. Characterization of Components and Compounds

This was obtained by analyzing the following:

1. Morphological characteristics:

- XRD: using a DRON 2.0 X-ray diffractometer, the variation at room temperature of the radial diffraction intensity dependence on the diffraction angle (2 theta) was recorded. The working conditions were a step size of 0.03° (2 theta), scanning rate = 8 s/step, filter with λ = 1.7921 Å, and a diffraction range of 2–15° (2 theta) for the small angles and 15–32° for the wide angles. The interbasal spacing was calculated based on the Bragg law (nλ = 2dsinθ, where n is an integer; λ is the wavelength of X-ray; d is the spacing between the planes in the atomic lattice; and θ is the angle between the incident ray and the scattering planes);
- Scanning electron microscopy, SEM, was performed on a VEGA TESTAN microscope at the tension of 30 kV. Before the examination at a 500× and 2000× resolution degree, the samples were cryogenically fractured into liquid nitrogen and then covered with a thin platinum layer.

2. Thermal behavior:
   - The DSC analysis under dynamic conditions was performed with Netzsch DSC 204 F1 Phoenix equipment by heating the samples from −30 °C to 100 °C to remove the thermal history, cooling them again to −30 °C, and heating them again to 200 °C with 10 °C/min under nitrogen (a 20 mL/min flow rate). This temperature range was chosen to highlight the 1st and 2nd transitions that occur before thermal degradation. The DSC included two heating steps in order to obtain the material characteristics reflected by the second heating run without the influence of any thermal history described by the first heating. The thermal analysis in the dynamic mode was performed to identify the material transitions and thermal degradation behavior (the beginning process temperature, number of degradation steps, etc.);
   - The DSC analysis under static conditions was carried out on the same DSC device by working at two temperatures, 140 °C and 200 °C, with dynamic heating up at these two temperatures with 10 °C/min after reaching the desired value the temperature was kept constant for 90 min at 140 °C or 200 °C. Under static conditions, the silicate was studied at 200 °C while the starch and PVOH were studied at 140 °C and 200 °C. The thermal analysis in the static mode was used to identify the thermal stability at a temperature of interest to avoid the degradation and so to choose the right compounding time;
   - A TGA (with dynamic conditions) was operated on a TGA Q500 system (TA Instruments, Linseis Messgeraete GmbH, Selb, Germany) under a nitrogen atmosphere. The samples were heated from room temperature to 800 °C at a heating rate of 10 °C/min and a nitrogen gas flow rate of 90 mL/min in the furnace. This temperature range was chosen to highlight the pyrolysis processes. The derivatives of the TGA curves were obtained using Universal 280 Analysis 2000, version 4 7 and Origin 2018 software.

3. The dynamic-mechanical properties were investigated with a DMA TRITEC 2000 B instrument (Triton Technologies) in a single cantilever mode from −60 to 100 °C with 1 Hz frequency and a 5 °C/min heating rate. During testing, the dynamic mechanical property parameters of the storage modulus, loss modulus, and loss factor were recorded from negative to positive temperatures in the ranges of interest for various applications starting from −25 °C to 160 °C.
4. Color: according to ASTM D6290-19.

3. Results and Discussion

3.1. Exfoliation of Silicate via Shear Stress during Melt Compounding (Figures 1–5)

Before melt compounding, the silicate and polymers were thermodynamically and morphologically characterized. The effect of the silicate delaminated in a Brabender plasticorder, reflected by the color of the obtained compound containing such silicate, can be explained by the thermal behavior of the nanofiller and the two polymers from the blend

and by the comparative analysis of the silicate morphology before and after delamination, as shown below.

The DSC thermogram of Nanocor I 28 in Figure 1a indicates an endothermic process in the temperature range up to 200 °C, which, according to the TGA registration (Figure 1b), involves a weight loss of 3–4% (usual conversion of mg to percentage), confirmed by the DTA data from the same Figure 1b.

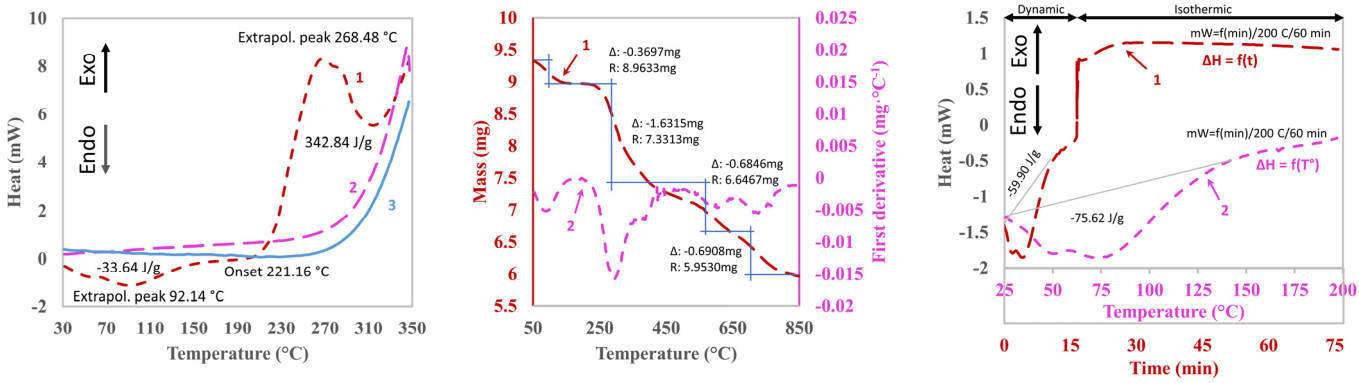

(**a**) (**b**) (**c**)

Figure 1. The thermal behavior of Nanocor I 28 in dynamic ((**a**) DSC thermogram; (**b**) TGA thermogram) and static ((**c**) isotherm at 200 °C) registrations; (**a**): 1—first heating; 2—cooling; 3—second heating; (**b**) 1—TGA curve; 2—DTA curve; (**c**) isothermal registration at 200 °C (1) after heating until 200 °C during the first 15 min in dynamic registration (Δ mass loss due to degradation and R_n mass associated with a decrease in the delta mass for each step (n^{th}) of degradation).

When the temperature increases, a second exothermic step of degradation begins at approximately 200 °C and ends at 430 °C when the weight loss is approximately 17.8%. This process has two stages, according to the TGA; the first one ends at approximately 310 °C, and the second one ends at 430 °C. Two other small degradations occur from 430 °C to 870 °C, corresponding to a weight loss of another 15% of the total weight of Nanocor I28 (Figure 1b). The stability of Nanocor I 28 at 200 °C was only for 2 min (Figure 1c), after which, in the isothermal registration of 60 min, a slight exothermic process occurred. According to Figure 1c, the heating of the sample up to the isothermal measurement temperature of 200 °C lasted for 15 min, after which the sample remained for another 60 min at 200 °C, during which no notable thermal effect occurred.

Later, after 90 min in the Brabender plasticorder at 200 °C under thermo-mechanical stress, the morphology of the layered silicate changed, reflected by a random variation of the crystal size (both by increasing with 11.02 Å for certain crystals and decreasing with 22.3 Å for others), slight movements towards higher values of the diffraction angles (0.05°–0.075°), slight increases in the diffraction intensities for certain crystals (almost 100 counts/s), and, most importantly, the disappearance of the small diffraction shoulder from 6.01° in the nanometric range, which can be found on the initial curve (Table 1, Figure 2).

Table 1. The effect of the Brabender plasticorder thermo-mechanical stress acting for 90 min on the morphology of the multilayered silicate, reflected by the initial process and after the pretreatment XRD diffractograms, i.e., I28-0 and I28-90, respectively.

I 28-0				I 28-90				Changes, I 28-90 Versus I 28-0			
2 θ, º	d, Å	Crystal Size, Å	Intensity, Counts/s	2 θ, º	d, Å	Crystal Size, Å	Intensity, Counts/s	2 θ, º	d, Å	Crystal Size, Å	Intensity, Counts/s
4.21	24.39	114.03	20.000	4.26	24.08	91.73	20.000	↑ 0.05	↓ 0.31	↓ 22.3	0
6.01	17.05	64.82	4000	-	-	-	-				
8.31	12.35	148.34	1.400	8.36	12.27	155.36	1.500	↑ 0.075	↓ 0.074	↑ 11.02	↑ 100

All these changes can be observed from the XRD diffractogram shape for the 90 min-treated multilayered silicates compared with that of the silicate without this treatment (Figure 2). In short, because the diffractogram after 90 min is wider than the initial one, it can be appreciated that after the treatment, more crystals with larger sizes are formed.

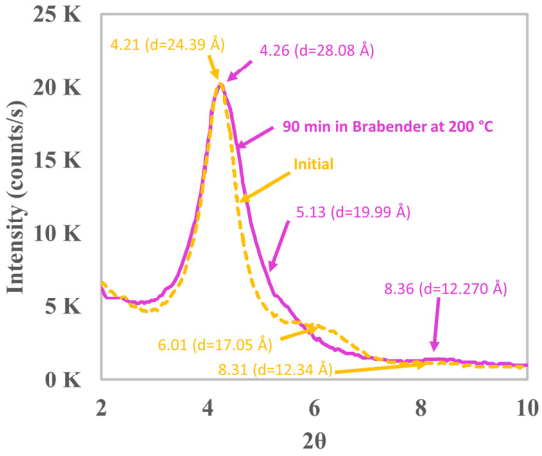

Figure 2. The influence of the thermo-mechanical treatment in a Brabender plasticorder on the Nanocor I 28 morphologies analyzed via X-ray diffraction (XRD); yellow: initial Nanocor I28 (I28-0); magenta: Nanocor I 28 after 90 min in the compounder (I 28-90).

Consequently, the mechano-thermal treatment of Nanocor I 28 in the Brabender plasticorder resulted in the overlapping of thermal processes of the desorption of water and the degradation of surfactant functional groups [47,48], which took place until 200 °C with a thermal degradation from 200 °C to 850 °C. Additionally, there was a mechanical process, which altered the silicate morphology (increasing the large crystal numbers, widening their size distribution, and causing the disappearance of a diffraction shoulder and uncontrolled variations in the interlamellar distance). All these processes generated modifications that did not favor polymeric nanocompositing. The thermal analysis in the dynamic mode for Nanocor I28 demonstrated its significant thermal instability and the analysis in the static mode proved that the thermal stability at the analyzed temperature was only 2 min. This thermal behavior in both the dynamic and static modes and the morphological changes observed in the performed XRD analysis prove that Nanocor I 28 cannot be exfoliated in the compounder.

The thermal behavior of starch was investigated in both dynamic (Figure 3a,b) and static conditions (Figure 3c,d).

The first heating curve of starch presents an endothermic transition, on the entire range of interest for melt compounding and up to 180 °C, involving a weight loss of 9%, which probably represents water evaporation (Figure 3a,b). This means that starch must be dried for certain formulations before melt compounding. As was already mentioned in Section 2.3, the information provided with the first DSC heating thermogram is not of interest to the analyzed subject because it is related to the thermal history of the sample under discussion. Similar situations can be found in Figures 1, 3 and 4.

The second heating curve shows a slight exothermic stage starting at 180 °C (Figure 3a), which intensifies around 250 °C and, up to 380 °C, it converts into a new degradation step characterized by a weight loss of 63% (Figure 3b). The degradation continues up to 520 °C when the starch loses almost its entire weight (98%). Starch displays a slightly exothermic process even under static conditions at 200 °C (Figure 3c) and 140 °C (Figure 3d), which show the high degradability of starch, which mainly undergoes breaks in the branches of amylopectin under thermo-mechanical conditions [49]. These results show that starch degrades at temperatures specific to melt processing, even in the static mode at 140 °C and 200 °C, respectively. Above 280 °C, condensation reactions occur between the attached hydroxyl groups of the neighboring chains with the formation of ether bonds. At higher

temperatures, the starch dextrinization occurs with the formation of levoglucosan and many different volatiles [50–55]. These results show that starch degrades at temperatures specific to melt processing, even in the static mode at 140 °C and 200 °C, respectively.

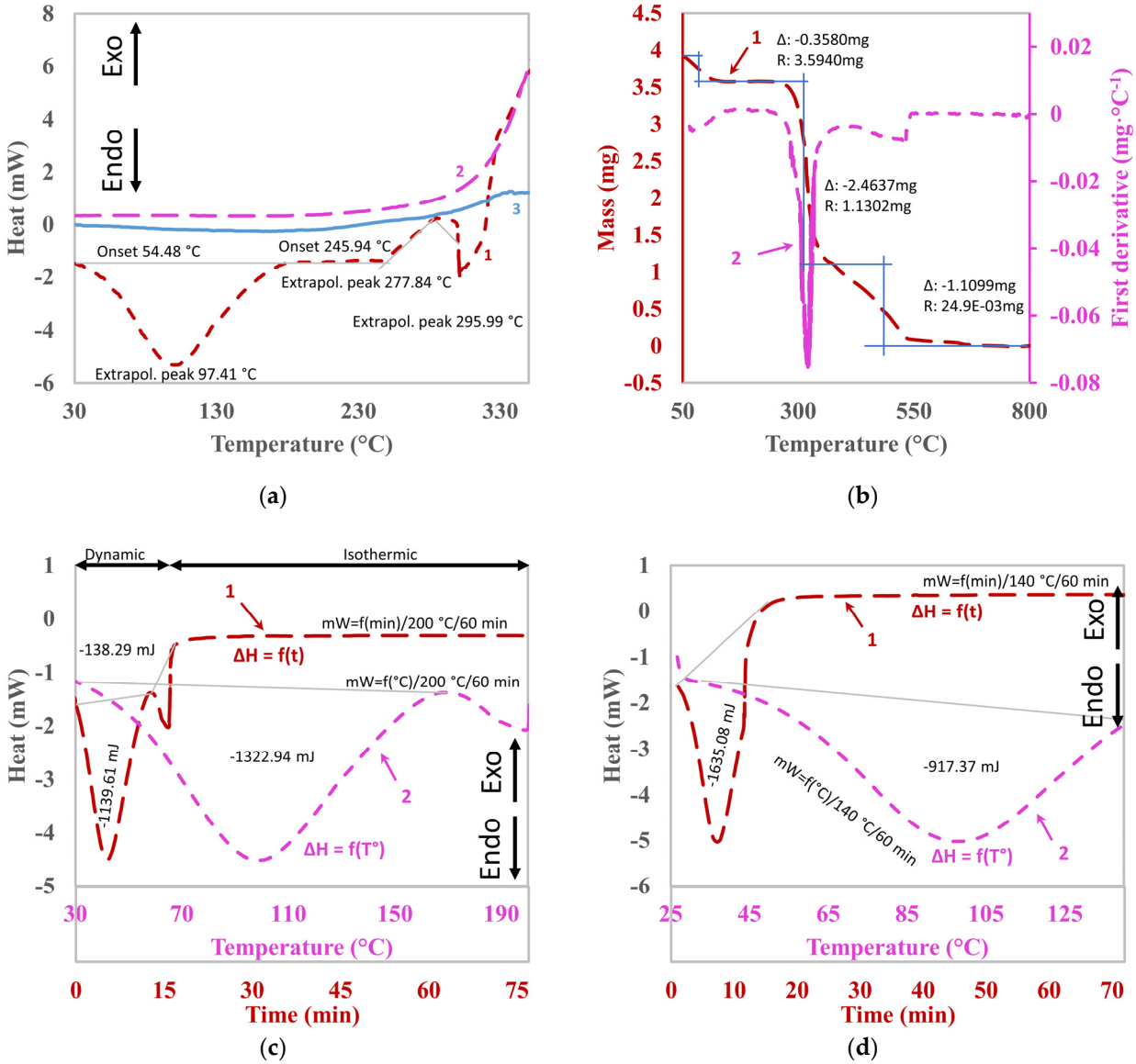

Figure 3. The thermal behavior of corn starch under dynamic: ((**a**) DSC thermogram; (**b**) TGA thermogram) and static ((**c**) isotherm at 200 °C; (**d**) isotherm at 140 °C) conditions; (**a**): 1—first heating; 2—cooling; 3—second heating; (**b**): 1—TGA curve; 2—DTA curve; (**c**) isothermal registration at 200 °C (1) after heating at 200 °C (2) which lasts for 15 min (1—dynamic registration); (**d**) isothermal registration at 140 °C (1) after heating at 140 °C (2) which lasts for 15 min (1—dynamic registration) (−Δ mass loss due to degradation; R_n mass associated with a decrease in the delta mass for each step (n^{th}) of degradation).

Starting from 40 °C and up to approximately 160 °C with a peak at 85.12 °C, PVOH undergoes an endothermic process of relatively intense evaporation (mainly water), losing approximately 5% of its weight (Figure 4a,b). From approximately 165 °C until 230 °C, it follows a second endothermic process with a maximum at 187.98 °C. From 238 °C and, respectively, 285 °C, two more degradation processes occur, one exothermic and the other one endothermic, which extended up to ~480 °C. After these two steps, PVOH loses almost 99% of its weight. It can be considered that the thermal effects described by the first recording under dynamic conditions impose the drying of the polymer before

melt compounding (Figure 4a). According to the DSC thermogram registered during the second heating under dynamic conditions (Figure 4b), PVOH degradation starts from approximately 140 °C. At this temperature under static conditions for 60 min, a slight exothermal increase can be immediately observed [41] (Figure 4c). This indicates that the polymer degrades even during the time when it is kept at a constant temperature of 140 °C. A similar exothermic increase in the heat flow, indicating PVOH degradation, takes place during it isothermal holding at 200 °C (Figure 4d), even from the beginning of the experiment and during the entire experimental time (of 60 min). These results were possible because of the PVOH degradation under 300 °C through water elimination, chain scission, and the formation of saturated and unsaturated aldehydes and ketone [41]. Between 300 °C and 850 °C, there is a PVOH carbonization with the formation of carbon structure and the elimination of heteroatoms and, therefore, the elimination of water, CO_2, CH_3CHO, and the later consecutive processes of aromatization, cyclization, and condensation [56].

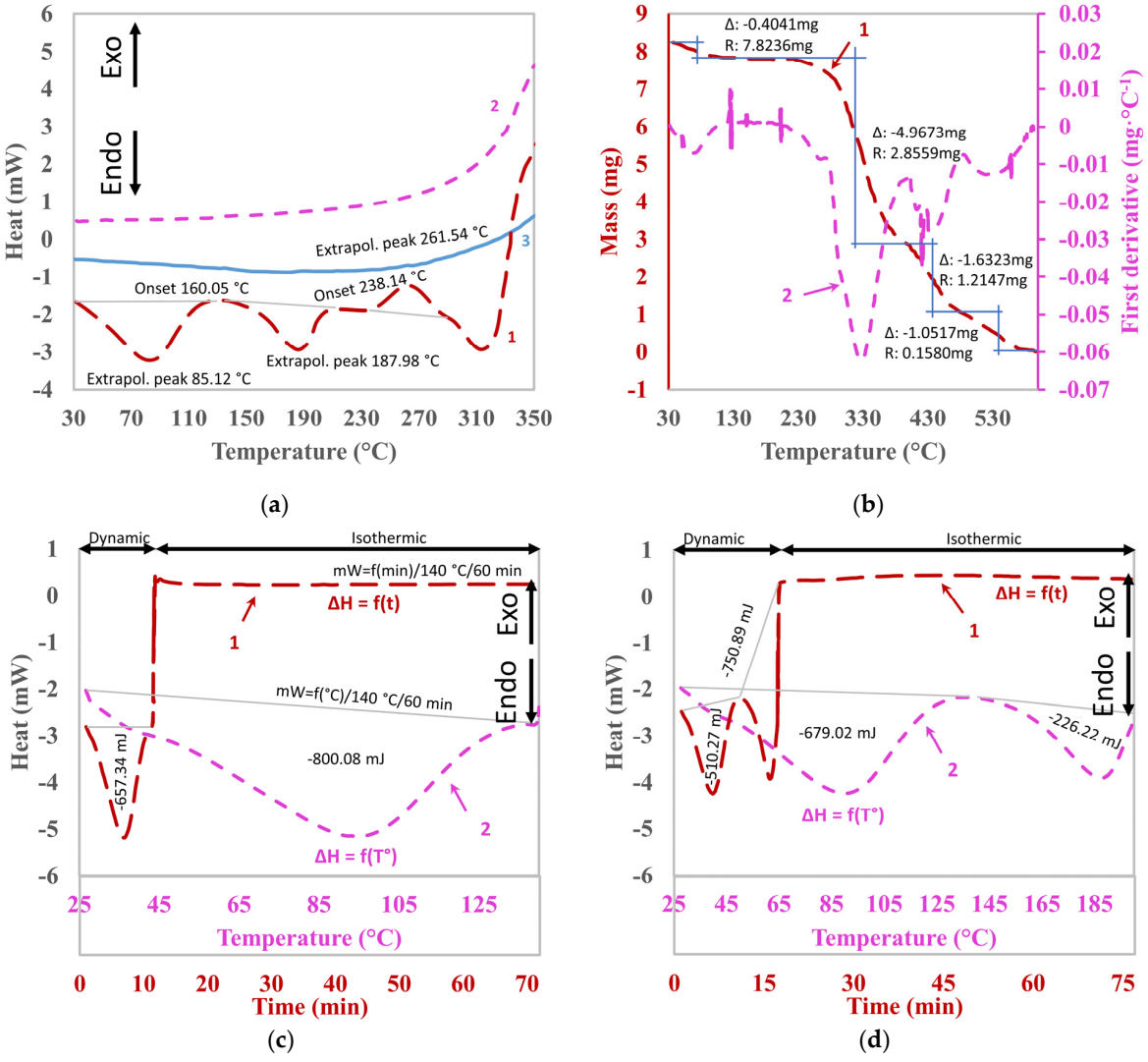

Figure 4. Thermal behavior of PVOH under dynamic ((**a**) DSC thermogram; (**b**) TGA thermogram) and static ((**c**) isotherm at 200 °C; (**d**) isotherm at 140 °C) conditions; (**a**): 1—first heating round; 2—cooling; 3—second heating round; (**b**): 1—TGA curve; 2—DTA curve; (**c**) isothermal registration at 200 °C (1) after heating at 200 °C (2) which lasts for 15 min (1—dynamic registration); (**d**) isothermal registration at 140 °C (1) after heating at 140 °C (2) which lasts for 15 min (1—dynamic registration); (Δ mass loss due to degradation and R_n mass associated with a decrease in the delta mass for each (n^{th}) step of degradation).

The embedding of 4% Nanocor I28 without prior delamination in a matrix with 70% starch and 30% PVOH for an increased compounding time of 30 min leads to a highly degraded, strongly colored compound with a degree of whiteness of 43.59% (Figure 5). This color is perfectly explained if the thermal behavior under dynamic and static conditions of all the components of the studied compounds described by the above-presented results and illustrated by Figures 1, 3 and 5, are considered. The continued action of temperature and shear stress degrades all of the components from the blend, starch, PVOH, and NaMMT. Furthermore, the loss of crystallized water by the silicate changes its morphology (Figure 2). The only conclusion of all of these results is that the layered silicates that are entangled into such matrices cannot be delaminated during melt compounding.

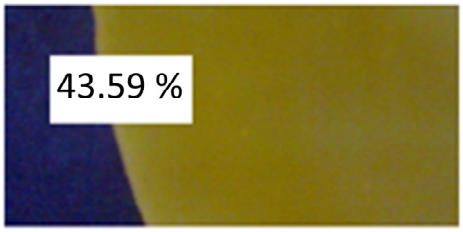

Figure 5. The change in the color of the starch-PVOH multilayered silicate during melt processing for 30 min in view of silicate delamination (yellow: color of the compound after 30 min in a Brabender plasticorder; the percent 43.59% represents the degree of whiteness; blue: support).

3.2. Pretreatment of the Multilayered Silicate before Melt Compounding (Figures 6–13)

The small-angle XRD diffractograms of the compounds containing the pretreated multilayered silicate under thermo-mechanical conditions at different times before its embedding into the melted starch-PVOH matrix shows a possible total exfoliation of NaMMT (Figure 6a, Table 2). With the increase in the pretreatment time of the silicate, the diffraction peaks move towards smaller angles, and their intensity decreases.

Table 2. The characteristics of the XRD diffractograms at small angles of the individual components and of the compounds with thermo-mechanically pretreated NaMMT at 50 °C before embedding into the starch-PVOH matrix.

Sample	2 θ, °	Intensity, Counts/s	Inter-Basal Spacing (d), Å
Materials			
NaMMT	6.93/3.01	100.47/98.14	5.35/12.77
Starch	10.03/15.35/17.41/20.04/23.29/30.05/43.36	225/525/570/405/148/75	7.99/5.9/5.2/4.9/4.7/4.5/3.9/3.7/3.36
PVOH	12.07/19.54/27.76/40.73	190/740/148/80	3.89/4.5/8.12
Compounds with NaMMT Thermo-mechanical pretreatment at 50 °C			
Time, h	**2 θ, °**	**Intensity, counts/s**	**Inter-basal spacing (d), Å**
8	6.93	32.3	29.21/-
16	6.99	24.03	29.08/-
24	6.53	42.55	29.09/-
72	4.84	41.66	29.21/-
288	4.38	35.22	30.21/-

Table 3 presents the results obtained from the silicate delamination under mechanical conditions alone, also in a process that preceded the melt compounding [46]. Comparing the results under mechanical and thermo-mechanical conditions, it can be concluded that the addition of temperature to the mechanical stress for the pretreatment renders the reduction of the electrostatic attractions between the silicate lamellae, improving the delamination degree and possibly inducing exfoliation. If the compounds containing NaMMT that are delaminated in mechanical conditions for 288 h have two diffraction maxima at theta angles of 4.63° and 9.57° with intensities of 53.64 counts/s and 28.10 counts/s, respectively, those

with preconditioned NaMMT under thermo-mechanical stress show a single diffraction angle of very low intensity, of approximately 42 counts/s even after 72 h of treatment (Tables 2 and 3). In the case of the compounds with thermo-mechanically treated silicate, the diffraction peak is shifted towards smaller angles, especially if the number of hours of treatment is higher (72 h) and has approximately 60% lower intensity than that of the untreated silicate. If the silicate is only mechanically pretreated, after 72 h, the diffraction intensity from the theta angle of 4.65° has practically the same intensity as the untreated silicate from 6.93° (Table 3). Because of the thermo-mechanical pretreatment, the silicate galleries are all uniform at approximately 29 Å, which means their enlargement is 2.27 and 1.5 times higher compared to the untreated and mechanically treated silicate, respectively (Tables 2 and 3).

Table 3. The characteristics of the XRD diffractograms at small angles of the compounds with mechanically pretreated NaMMT before incorporating them into the starch-PVOH matrix [46].

Time, h	2 θ, °	Intensity, Counts/s	Inter-Basal Spacing (d), Å
0	4.70/9.44	154.95/67.78	18.80/9.37
8	4.72/9.47	229.27/67.34	18.70/9.34
16	4.77/9.58	160.18/65.45	18.52/9.23
24	4.68/9.37	147.83/54.99	18.90/9.44
72	4.65/9.32	110.93/51.72	19.00/9.49
288	4.63/9.57	53.64/28.10	9.24

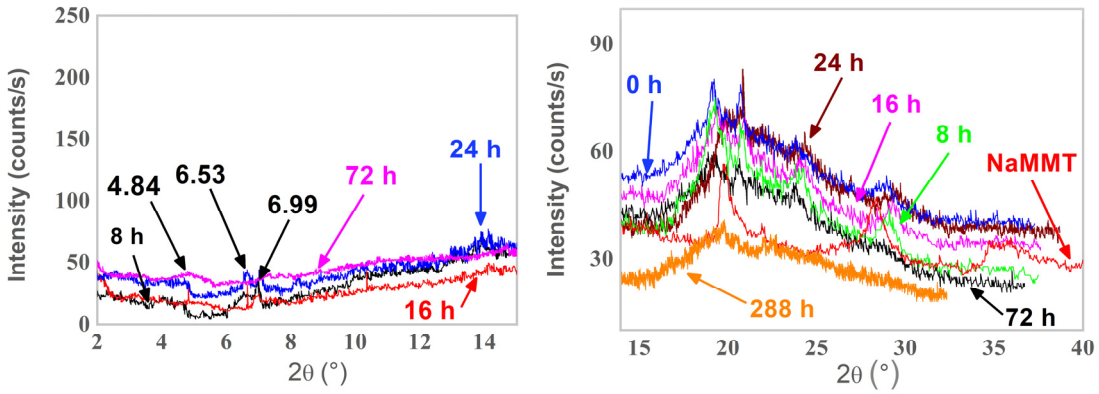

Figure 6. XRD diffractograms of the compounds with thermo-mechanically pretreated NaMMT before melt compounding with starch and PVOH ((**a**) slight angle; (**b**) wide angles).

The XRD results related to the compounds containing thermo-mechanical preconditioned silicate are even more interesting in comparison with the individual polymers starch, PVOH, and NaMMT (Figures 6 and 7, Tables 2 and 3). If the diffraction intensities of the starch are placed in the range of 148–525 counts/s for starch and, 80–740 counts/s for PVOH, and approximately 100 counts/s for NaMMT, all the compounds containing thermo-mechanically treated NaMMT before incorporation have only a single diffraction angle placed in the nanometric range, which does not have an intensity higher than 42.55 counts/s (Figures 6 and 7, Tables 2 and 3). In the case of the mechanically pretreated silicate in the same nanometric field, the new compounds have diffraction intensities higher than 100 counts/s, even up to 229.72 counts/s. The diffraction intensity for these compounds decreases only at very long pretreatment times of 255 h (Table 3) [46]. The inter-basal spacing of the thermo-mechanically and mechanically preconditioned silicates increases by approximately 3 and 1.5 times compared to the individual components. The pretreatment for delamination under thermo-mechanical conditions has a beneficial effect on the morphologies of new compounds as a whole, as also reflected by the wide-angle X-ray diffraction results (Figure 7). In the field of wide angles, the increase in the treatment

time decreases the number of theta angles at which the diffraction occurs from a total of thirteen angles for the three components (seven for starch, four for PVOH, and two for silicate) to three such angles for the compounds containing treated silicate. In conclusion, at both low and wide angles, the diffractions of the new compounds with pretreated silicate (thermo-mechanically or mechanically treated) differ from those of the individual components. It can be stated that long thermo-mechanical pretreatment times decrease the number of diffraction angles (Figure 6, Tables 2–4). From the seven diffraction peaks of starch, four of PVOH, and two of silicate after 288 h of pretreatment, the thermo-mechanically pretreated compound has diffractions at only three angles with values different from those of the individual components (Tables 2 and 4).

Table 4. The diffractometric characteristics at wide angles of compounds with thermo-mechanically pretreated NaMMT at 50 °C before embedding into the starch matrix.

Pre-Treatment Time, h	2 θ, °	Intensity, Counts/s
0	19.22/20.85/21.92/23.77/28.8	80/83/67.71/63.63/49.3
8	19.13/20.9/23.85/29.03	73.13/69.21/56.09/44.17
16	19.81/20.79/23.77/278.8	80/83/67.71/63.63/49.3
24	19.41/20.82/24/29.26	64.65/83/62.27/50.72
72	19.02/20.42/23.74	58/56/50
288	16.63/19.06/22	23.9/39.62/35

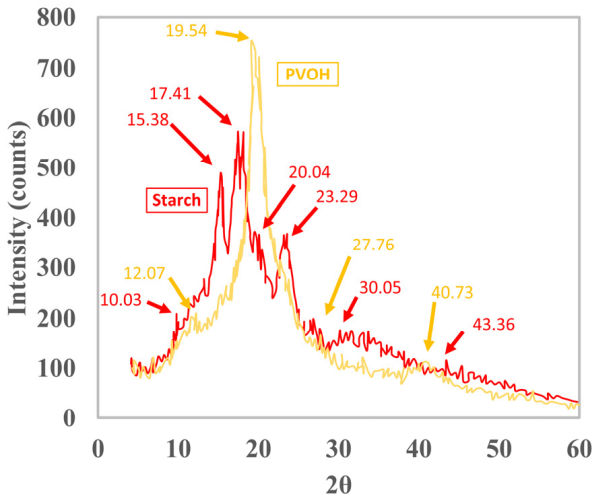

Figure 7. X-ray diffractions of starch (red) and PVOH (yellow).

The pretreatment of the multilayered silicate compound through thermo-mechanical stirring in a common plasticizer for both starch and PVOH improves the dynamic-mechanical properties of the compounds into which the silicate was embedded. This influence is more obvious, the more the delamination advances (Figure 8).

The compound containing silicate that is thermo-mechanically pretreated for 72 h has a 3.5 times higher storage modulus and 2.6 times increased loss modulus compared to the compound containing untreated silicate (Figure 8a,b).

The storage modulus measures the stored energy before breaking, describing the elastic behavior, while the loss modulus measures the dissipated energy as heat and describes the viscous behavior [57]. The dissipation factor (tag delta: the ratio between the viscous and the elastic response [58]) has small values of a maximum of 5 if the silicate is thermo-mechanically treated for 72 h and much higher values of 10–83 (Figure 8c) if the silicate is treated for 24 h (Figure 8c). Overall, the material has a higher elastic deformation

ability with increased silicate exfoliation compared to those of compounds containing only mechanically pretreated silicate.

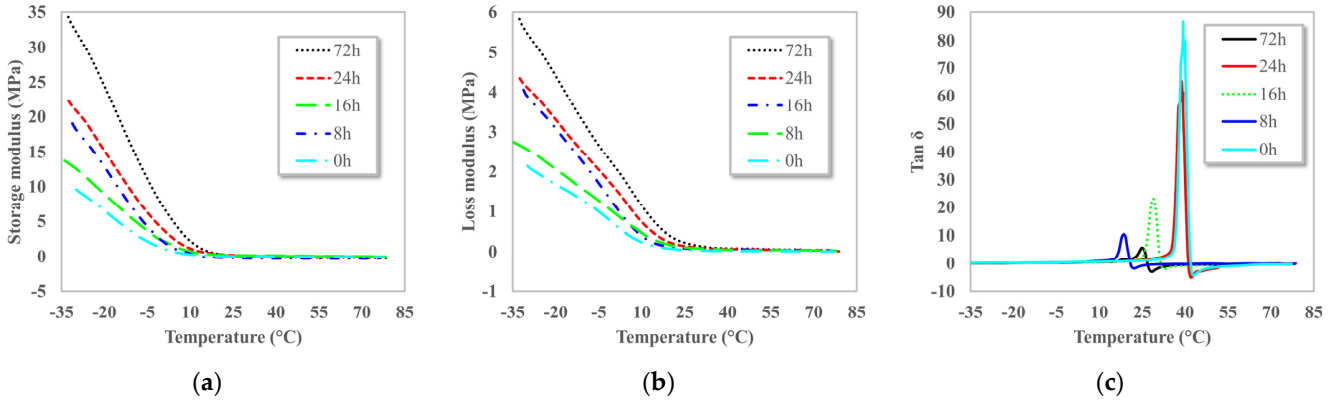

Figure 8. The dynamic and mechanical properties at 0.316 Hz of the starch-PVOH compounds containing thermo-mechanically pretreated NaMMT: (**a**) storage modulus; (**b**) loss modulus; (**c**) dissipation factor.

The benefit is even more obvious if the dynamic and mechanical properties of the silicate compounds (Figure 8) are compared with those of the silicate-free compounds (Figure 9). As it appears in Figure 9, if the starch-PVOH compounds do not contain silicate, depending on the plasticization level, they have a storage modulus from 0.01 to 2 MPa, a loss modulus in the range of 0.05–0.75 MPa, and a tan delta between 2 and 20 at −20 °C, which is much lower than in the case of compounds with silicate (Figure 8). If the compounds that do not contain silicate are compared (Figure 9), then the increase in the elastic deformation capacity of the compounds with thermo-mechanically treated silicate for 72 h (Figure 8) is approximately 17 times higher, and the number of defects is only 10 times greater (comparisons for values registered at −20 °C).

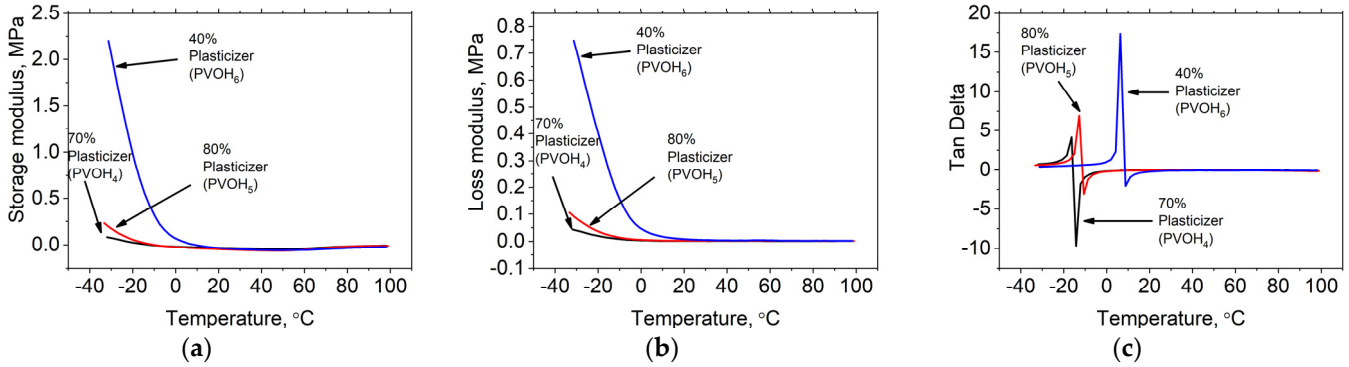

Figure 9. The dependence of the dynamic and mechanical properties of the starch-PVOH compounds on the plasticization degree at 0.316 Hz ((**a**) storage modulus; (**b**) loss modulus; (**c**) dissipation factor).

The incorporation of thermo-mechanically pretreated layered silicate into starch-PVOH matrices also generates an improvement in the thermal behavior (Figure 10).

If the number of degradation steps of the individual components (Figures 3 and 4) are compared with those characterizing the compounds with thermo-mechanical preconditioned silicate (Figure 10), according to the TGA curve, the thermal degradation of the new blends follows one main large step as opposed to 3–4 for all the three components of the compounds. The most likely explanation is related to the good interface agent role of the silicate lamellae at the interface between the two polymers. These results were also confirmed with the SEM results presented below. However, on the DTA curve, small intermediate degradation processes of very low intensity can be observed. These processes

are rather heterogeneous and most likely are related to the water brought into the system by the silicate that has been thermo-mechanically treated in advance, before embedding.

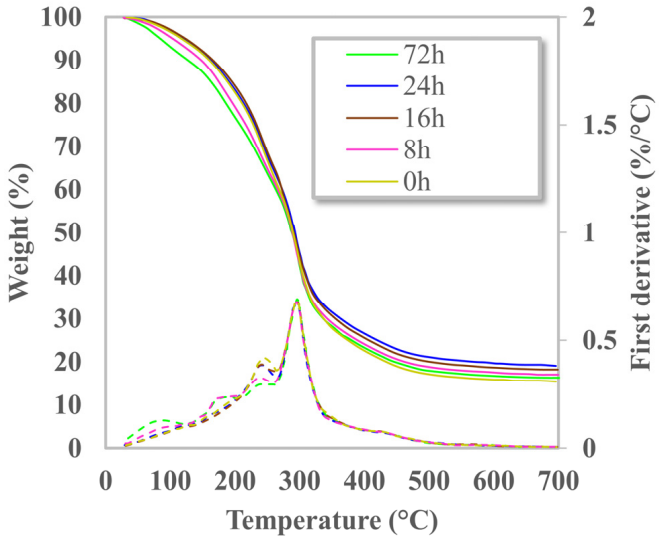

Figure 10. Degradation steps of a blend with a 70% starch/30% PVOH matrix, and 4% thermo-mechanically treated NaMMT.

The main difference between the temperatures from the beginning of the thermal degradation of the individual components (Figures 1, 3, 4 and 11a) and those of the compounds containing thermo-mechanically pretreated silicates (Figure 11b,c) is an increase in the starting degradation temperatures with almost 30 °C–50 °C. From these figures, it can be seen that the individual components start to degrade in the 150 °C–200 °C temperature range (192 °C: Nanocor I 28 (Figure 1a,b), 180 °C: starch (Figure 3a,b), 150 °C: PVOH (Figure 4a,b)) whereas the compounds containing thermo-mechanically treated filler, depending on the exfoliation degree of the silicate, are in the range from 230 °C to 250 °C (Figure 11).

That is why the incorporation of this type of silicate via melt compounding must be carried out only in starch-PVOH matrices that can be compounded at temperatures that are not higher than 110 °C–120 °C, as is explained below. Otherwise, the hydration water brought into the system by the preconditioning silicate is lost, which is not desirable, as it is a good plasticizer for the two polymers. In addition, if there is no need to use another plasticizer due to the hydration water, it also presents the advantage of considerably reducing the compound's cost.

The temperatures at which the thermal degradation of the individual components begins (Figure 11a) are slightly lower than those of the starch-PVOH compounds that contain NaMMT that was not pretreated and were melt compounded for 30 min (Figure 11b). If, however, the compounds that contain thermo-mechanically preconditioned silicate are compared, an increase of 30 °C–50 °C of this temperature is found, as mentioned above (Figure 11c).

The SEM micrographs shown in Figure 12 prove the role of thermo-mechanically preconditioned silicates as an interface agent between the phases of the PVOH-starch blends. The compound without silicate (Figure 12a) has an irregular structure, with discontinuities most probably due to the impossibility of dispersing some linear macromolecules of amylose and PVOH into the other macromolecules shaped as clusters of amylopectin. The presence of silicate homogenizes the morphology, which becomes more homogeneous the longer the thermo-mechanical pretreatment (Figure 12b–e).

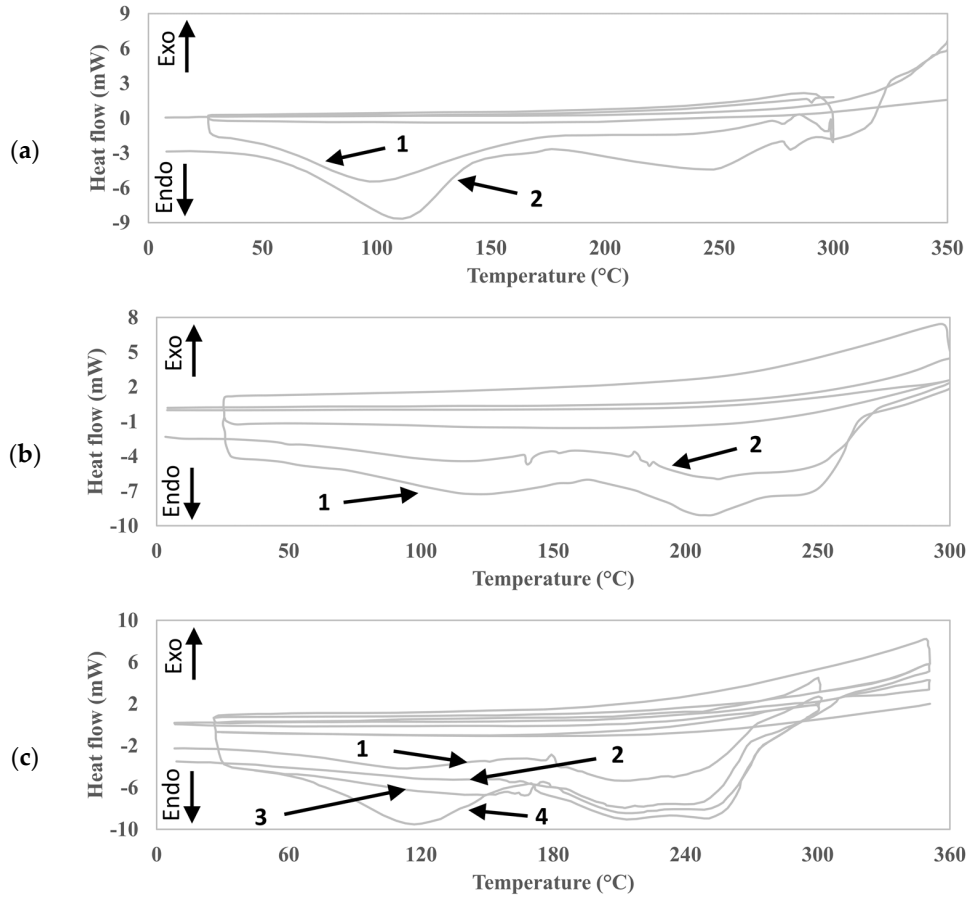

Figure 11. Comparison of the DSC thermograms of the individual components (**a**) curve 1: starch, curve 2: PVOH; (**b**) curve 1: without silicate, curve 2: untreated; (**c**) thermo−mechanically treated for a different time (**c**); 1—8 h, 2—16 h, 3—24 h, and 4—72 h.

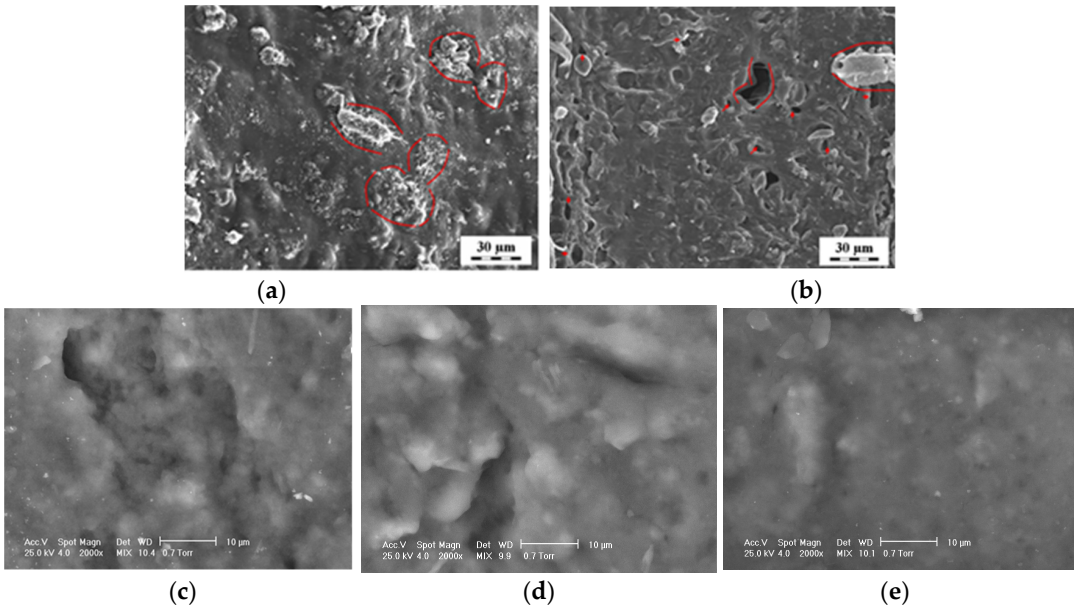

Figure 12. The SEM micrographs of starch-PVOH compounds with 4% thermo-mechanically preconditioned layered silicate: (**a**) a compound without silicate; (**b**) a compound with 4% untreated silicate; (**c**) a compound with 4% pretreated silicate for 8 h; (**d**) a compound with 4% pretreated silicate for 24 h; (**e**) a compound with 4% pretreated silicate for 72 h.

The embedding of multilayered thermo-mechanically pretreated silicate into a starch-PVOH matrix resulted in a white nanocomposite (Figure 13), which, according to the XRD results, has an intercalated-exfoliated structure. The advantage of the thermo-mechanical pretreatment of the silicate before melt compounding can be observed by comparing the color of this compound with that of the compound with the same amount of silicate but which, for the purpose of delamination, was kept in a compounder for 30 min (Figure 5).

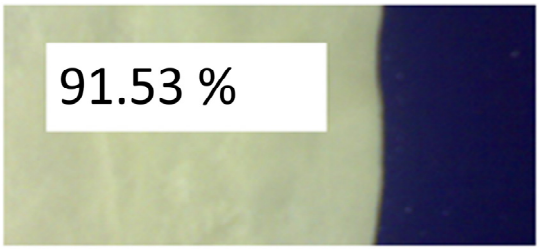

Figure 13. A nanocomposite with 70% starch, 30% PVOH, and a 4% 28-h thermo-mechanically pretreated silicate; (white: color of the compound; 91.53% represents the degree of whiteness; blue: support).

The delamination of the montmorillonite and the uniform dispersion of the resulting lamellae into the polymer matrix represent the main requirement to be fulfilled for obtaining nanocomposites using these two polymers, PVOH, and starch. Initially, the dispersion of the layered silicate during compounding in the melt should be extremely efficient. The use of this method for the purpose of exfoliating silicates with the help of shearing forces during compounding is limited by the thermostability of the polymers, the additives, and the other materials with which the modification was completed. Increasing the compounding time causes the starch-PVOH blend to turn yellow. The achievement of exfoliated and intercalated nanocomposites via this method is limited by the high degree of degradability of the thermo-mechanical conditions of these types of polymers. Due to the degradation of starch and PVOH and due to the loss of the specific hydration water from the silicate, the delamination cannot be performed during melt processing. The morphological changes of the multilayered silicate into the thermo-mechanical environment from the compounder (Brabender plasticorder) do not favor nanocompositing because of the unfavorable changes (the appearance of new crystals, the movement of the diffraction towards higher angles, the increase in certain crystal sizes, and the increase in the diffraction intensity), which have a higher impact than the favorable ones (the decrease in the size of some crystals however in competition with the reverse process of increasing the size of the crystals).

In previous works, water was used as a plasticizer, and it was proven to be a good plasticizer for blends based on starch and polyvinyl [59–63]. The interaction of montmorillonite with water is common to all silicates and includes the following stages: hydration, dispersion, flocculation, deflocculation, and aggregation [64,65]. The water molecules can penetrate between the silicate layers, leading to swelling, thus increasing the distance between the MMT lamellae [66]. Due to the diffusion and osmosis processes, the silicate lamellae move further and further apart until individual lamellae are obtained (Figure 2). In the dry state, the platelets are "face to face" like playing cards in a pack. Hydration occurs when the silicate packs absorb water and swell. Dispersion or disaggregation represents the collapse of the "lamellar edifice" due to the loss of attractive forces between the plates under the action of water (very high dielectric constant). During this process it became evident that the absorption of water by sodium-montmorillonite seems to be controlled by the competition for the formation of hydrogen bonds between the water molecules and the silicate tetrahedra. A small degree of exfoliation of the silicate can be a sign that the plasticizer has not sufficiently interacted with the layered silicate and therefore has not dispersed [37]. If the silicate is treated for a longer time, then the XRD diffractograms show the spacing of the NaMMT lamellae, even their exfoliation, the major disadvantage being the long pretreatment time [46]. If the stirring of NaMMT is performed in hot water

(50 °C), it was found that, because of the temperature, the diffraction peak from 4.63° 2 theta of the nanocomposite has a 22% lower intensity than the similar absorption from the nanocomposite which only contains mechanically pretreated silicate [35]. This effect was obtained after only 72 h in the first case compared to 288 h for the second situation.

The pretreatment at 50 °C shortened by four times the period to obtain the same type of nanocomposites, which are characterized by very low diffraction intensities between 24.03 counts/s and 42.55 counts/s. It was observed that the diffractions of the nanocomposites did not occur at the specific angles of the layered silicate but were close to those found for the compound without silicate, slightly shifting towards smaller diffraction angles. Their intensities were up to 73% lower in the case of treatment in water at 50 °C, and 65% lower if the treatment was carried out at room temperature with stirring. In contrast to the treatment at room temperature, which provided two diffraction angles, one of low intensity at approximately 9.4° and another narrower one at approximately 4.6°, the treatment at 50 °C only induced one diffraction peak at angles placed in the range of 6.99–4.63°. In addition to the mechanical action, the temperature helps to overcome the electrostatic forces between the lamellae because it increases the energy of movement and favors new intermolecular arrangements. In short, the proven properties of the new materials are: an elastic behavior 3.5 times higher than the similar ones of the systems only treated mechanically, a smaller defect number, and a higher dissipation capacity of the deformation energy. The temperature at which the degradation of these nanocomposites begins is 30 °C–50 °C higher than the temperatures at which the degradations of the individual components begin. In addition, the morphological structure is uniform without the void-like defects found in the compounds without silicates. The pretreated silicate can be incorporated only in starch-PVOH matrices with formulations that can be melt-compounded at 110 °C–120 °C.

4. Conclusions

To achieve new nanocomposites with starch-based matrices, this article compared two exfoliation options of multilayered silicate, one considering the shear stress and temperature during melt compounding and another via thermo-mechanically pretreating a multilayered silicate in a plasticizer (water) common to the two polymers from the compound, starch, and polyvinyl alcohol, pretreatment performed before the melt compounding.

The results proved that it was possible to cancel the electrostatic attractions between the lamellae of a multilayered silicate such that, during its melt compounding with the starch-PVOH matrix, new attractions between the individual lamellae thus obtained and the polar groups of each polymer from the blend were settled. This determined the formation of exfoliated-intercalated nanocomposites.

The pretreatment of silicate in a plasticizer common to the two polymers from the blend means the removal of other plasticizers from the typical formulations of such blends and obtaining materials with improved properties of practical impact and convenient cost.

The silicate exfoliation obtained by increasing the action time of the shear stress and temperature in a melt compounding device proved to be an ineffective method for silicate exfoliation following the high degradability of starch and PVOH and the loss of hydration water by the multilayered silicate.

Author Contributions: Conceptualization, D.D.; methodology, D.D., R.M.G., B.T., C.-M.D., E.V., R.T. and C.-A.N.; validation: D.D., R.M.G., B.T., C.-M.D., E.V., R.T. and C.-A.N.; investigation, D.D., R.M.G., B.T., C.-M.D., E.V., R.T. and C.-A.N.; resources, D.D., D.C.-A. and F.O.; data curation, D.D., B.T., D.C.-A. and C.-A.N.; writing—original draft preparation, D.D. and B.T.; writing—review and editing, D.D., B.T., D.C.-A. and F.O.; visualization, B.T. and D.C.-A.; supervision, D.D. and F.O.; project administration, D.D., D.C-A. and F.O.; funding acquisition, D.D. and F.O. All authors have read and agreed to the published version of the manuscript.

Funding: This research was funded by the PN 23.06 Core Program-Chem NewDeal within the National Plan for Research, Development, and Innovation 2022–2027, developed with the support of the Ministry of Research, Innovation, and Digitization, project no. PN 23.06.02.01 InteGral and

by project POC-A1-A1.2.3-G-2015-P_40_352, My_SMIS 105684, subsidiary projects 1480/2019 and 1488/2020, European Regional Development Fund (ERDF), the Competitiveness Operational Program (POC), Axis 1.

Data Availability Statement: The data are contained within the article.

Acknowledgments: The authors thank their colleague Florentina-Simona Maica for the thermal characterization of the materials used. The authors acknowledges support from project 15 PFE NeXT-Bexcel. D.D. also acknowledges support from contract 59/2016 and contract nr. 32-101.

Conflicts of Interest: The authors declare no conflicts of interest. The funders had no role in the design of the study; in the collection, analyses, or interpretation of data; in the writing of the manuscript; or in the decision to publish the results.

References

1. Ming, Y.; Zhou, Z.; Hao, T.; Nie, Y. Polymer Nanocomposites: Role of modified filler content and interfacial interaction on crystallization. *Eur. Polym. J.* **2022**, *162*, 110894. [CrossRef]
2. Zaikov, G.E.; Thomas, S. Progress in polymer nanocomposite research. In *Progress in Polymer Nanocomposite Research*; Nova Science Pub Inc.: Hauppauge, NY, USA, 2008; pp. 1–415.
3. Mai, Y.W.; Yu, Z.Z. *Polymer Nanocomposites*; Woodhead Publishing Ltd.: Cambridge, UK, 2006.
4. Knite, M.; Teteris, V.; Polyakov, B.; Erts, D. Electric and elastic properties of conductive polymeric nanocomposites on macro-and nanoscales. *Mater. Sci. Eng. C* **2002**, *19*, 15–19. [CrossRef]
5. Mao, L.; Imam, S.; Gordon, S.; Cinelli, P.; Chiellini, E. Extruded cornstarch-glycerol-polyvinyl alcohol blends: Mechanical properties, morphology, and biodegradability. *J. Polym. Environ.* **2000**, *8*, 205–211. [CrossRef]
6. Müller, K.; Bugnicourt, E.; Latorre, M.; Jorda, M.; Echegoyen Sanz, Y.; Lagaron, J.M.; Miesbauer, O.; Bianchin, A.; Hankin, S.; Bölz, U. Review on the processing and properties of polymer nanocomposites and nanocoatings and their applications in the packaging, automotive and solar energy fields. *Nanomaterials* **2017**, *7*, 74. [CrossRef]
7. Iroegbu, A.O.C.; Ray, S.S. Recent developments and future perspectives of biorenewable nanocomposites for advanced applications. *Nanotechnol. Rev.* **2022**, *11*, 1696–1721. [CrossRef]
8. Khan, I.; Khan, I.; Saeed, K.; Ali, N.; Zada, N.; Khan, A.; Ali, F.; Bilal, M.; Akhter, M.S. Polymer nanocomposites: An overview. *Smart Polym. Nanocomposites* **2023**, 167–184. [CrossRef]
9. Zare, Y. Recent progress on preparation and properties of nanocomposites from recycled polymers: A review. *Waste Manag.* **2013**, *33*, 598–604. [CrossRef] [PubMed]
10. Tang, X.; Alavi, S.; Herald, T.J. Effects of plasticizers on the structure and properties of starch–clay nanocomposite films. *Carbohydr. Polym.* **2008**, *74*, 552–558. [CrossRef]
11. Wang, N.; Zhang, X.; Han, N.; Bai, S. Effect of citric acid and processing on the performance of thermoplastic starch/montmorillonite nanocomposites. *Carbohydr. Polym.* **2009**, *76*, 68–73. [CrossRef]
12. Russo, M.A.L.; Truss, R.; Halley, P.J. The enzymatic hydrolysis of starch-based PVOH and polyol plasticised blends. *Carbohydr. Polym.* **2009**, *77*, 442–448. [CrossRef]
13. Rzaev, Z.M.O.; Yilmazbayhan, A.; Alper, E. A one-step preparation of compatibilized polypropylene-nanocomposites by reactive extrusion processing. *Adv. Polym. Technol.* **2007**, *26*, 41–55. [CrossRef]
14. Darder, M.; Aranda, P.; Ruiz-Hitzky, E. Bionanocomposites: A new concept of ecological, bioinspired, and functional hybrid materials. *Adv. Mater.* **2007**, *19*, 1309–1319. [CrossRef]
15. Utracki, L.A. Polymer Blends' Technology for Plastics Recycling. In *Frontiers in the Science and Technology of Polymer Recycling*; Springer: Berlin/Heidelberg, Germany, 1998; pp. 123–152.
16. Utracki, L.A. *Polymer Alloys and Blends: State of the Art*; National Research Council Canada, Industrial Materials Institute: Boucherville, QC, Canada, 1991.
17. Ishida, H. Miscibility. In *Encyclopedia of Polymer Science and Engineering*; John Wiley &Sons.Inc.: Hoboken, NJ, USA, 1989.
18. Fernández, M.L. Demixing in polymer blends. *Sci. Prog.* **1990**, *74*, 257–277.
19. Strobl, G.R. Concepts for understanding their structures and behaviour. *Phys. Polym.* **1996**, 349–385.
20. Utracki, L.A. *Clay-Containing Polymeric Nanocomposites*; iSmithers Rapra Publishing: Shrewsbury, UK, 2004; Volume 1.
21. Koo, J.H. *Polymer Nanocomposites: Processing, Characterization, and Applications*; McGraw-Hill Education: New York, NY, USA, 2006.
22. Alexandre, M.; Dubois, P. Polymer-layered silicate nanocomposites: Preparation, properties and uses of a new class of materials. *Mater. Sci. Eng. R Rep.* **2000**, *28*, 1–63. [CrossRef]
23. Fu, S.; Sun, Z.; Huang, P.; Li, Y.; Hu, N. Some basic aspects of polymer nanocomposites: A critical review. *Nano Mater. Sci.* **2019**, *1*, 2–30. [CrossRef]
24. Rivadeneira-Velasco, K.E.; Utreras-Silva, C.A.; Díaz-Barrios, A.; Sommer-Márquez, A.E.; Tafur, J.P.; Michell, R.M. Green nanocomposites based on thermoplastic starch: A review. *Polymers* **2021**, *13*, 3227. [CrossRef]

25. de Freitas, A.d.S.M.; da Silva, A.P.B.; Montagna, L.S.; Nogueira, I.A.; Carvalho, N.K.; de Faria, V.S.; Dos Santos, N.B.; Lemes, A.P. Thermoplastic starch nanocomposites: Sources, production and applications–a review. *J. Biomater. Sci. Polym. Ed.* **2022**, *33*, 900–945. [CrossRef] [PubMed]
26. Zakaria, N.H.; Muhammad, N.; Abdullah, M. Potential of starch nanocomposites for biomedical applications. *IOP Conf. Ser. Mater. Sci. Eng.* **2017**, *209*, 012087. [CrossRef]
27. Othman, N.; Azahari, N.A.; Ismail, H. Thermal properties of polyvinyl alcohol (PVOH)/corn starch blend film. *Malays. Polym. J.* **2011**, *6*, 147–154.
28. Sadhu, S.D.; Soni, A.; Garg, M. Thermal studies of the starch and polyvinyl alcohol based film and its nano composites. *J. Nanomedic. Nanotechnol. S* **2015**, *7*, 002. [CrossRef]
29. Kumar, S.V.; George, J.; Sajeevkumar, V.A. PVA based ternary nanocomposites with enhanced properties prepared by using a combination of rice starch nanocrystals and silver nanoparticles. *J. Polym. Environ.* **2018**, *26*, 3117–3127. [CrossRef]
30. Jagadeesh, P.; Puttegowda, M.; Mavinkere Rangappa, S.; Siengchin, S. Influence of nanofillers on biodegradable composites: A comprehensive review. *Polym. Compos.* **2021**, *42*, 5691–5711. [CrossRef]
31. Zanela, J.; Casagrande, M.; Shirai, M.A.; Lima, V.A.d.; Yamashita, F. Biodegradable blends of starch/polyvinyl alcohol/glycerol: Multivariate analysis of the mechanical properties. *Polimeros* **2016**, *26*, 193–196. [CrossRef]
32. Dimonie, D.; Petrache, M.; Damian, C.; Anton, L.; Musat, M.; Dima, Ş.-O.; Jinescu, C.; Maria, R. New evidences on the process sensitivity of some renewable blends based on starch considering their melt rheological properties. *Int. J. Polym. Sci.* **2016**, *2016*, 7873120. [CrossRef]
33. Rahman, W.; Sin, L.T.; Rahmat, A.R.; Samad, A.A. Thermal behaviour and interactions of cassava starch filled with glycerol plasticized polyvinyl alcohol blends. *Carbohydr. Polym.* **2010**, *81*, 805–810. [CrossRef]
34. Dimonie, D.; Damian, C.; Trusca, R.; Rapa, M. Some aspects conditioning the achieving of filaments for 3D printing from physical modified corn starch. *Mater. Plast.* **2019**, *56*, 351–359. [CrossRef]
35. Bangar, S.P.; Purewal, S.S.; Trif, M.; Maqsood, S.; Kumar, M.; Manjunatha, V.; Rusu, A.V. Functionality and applicability of starch-based films: An eco-friendly approach. *Foods* **2021**, *10*, 2181. [CrossRef] [PubMed]
36. Taguet, A.; Cassagnau, P.; Lopez-Cuesta, J.M. Structuration, selective dispersion and compatibilizing effect of (nano)fillers in polymer blends. *Prog. Polym. Sci.* **2014**, *39*, 1526–1563. [CrossRef]
37. Dimonie, D.; Radovici, C.; Trandafir, I.; Pop, S.F.; Dumitriu, I.; Fierascu, R.; Jecu, L.; Petrea, C.; Zaharia, C.; CoŞErea, R. Some aspects concerning the silicate delamination for obtaining polymeric bio-hybrids based on starch. *Rev. Roum. De Chim.* **2011**, *56*, 685–690.
38. Xie, F.; Pollet, E.; Halley, P.J.; Avérous, L. Starch-based nano-biocomposites. *Prog. Polym. Sci.* **2013**, *38*, 1590–1628. [CrossRef]
39. Mousa, M.; Dong, Y. The role of nanoparticle shapes and structures in material characterisation of polyvinyl alcohol (PVA) bionanocomposite films. *Polymers* **2020**, *12*, 264. [CrossRef]
40. Navarchian, A.H.; Jalalian, M.; Pirooz, M. Characterization of starch/poly (vinyl alcohol)/clay nanocomposite films prepared in twin-screw extruder for food packaging application. *J. Plast. Film Sheeting* **2015**, *31*, 309–336. [CrossRef]
41. Guarás, M.P.; Ludueña, L.N.; Alvarez, V.A. Recent advances in thermoplastic starch biodegradable nanocomposites. In *Handbook of Nanomaterials and Nanocomposites for Energy and Environmental Applications*; Springer: Cham, Switzerland, 2020; pp. 1–24.
42. Woldemariam, M.H.; Belingardi, G.; Koricho, E.G.; Reda, D.T. Effects of nanomaterials and particles on mechanical properties and fracture toughness of composite materials: A short review. *AIMS Mater. Sci.* **2019**, *6*, 1191–1212. [CrossRef]
43. Gamage, A.; Thiviya, P.; Mani, S.; Ponnusamy, P.G.; Manamperi, A.; Evon, P.; Merah, O.; Madhujith, T. Environmental properties and applications of biodegradable starch-based nanocomposites. *Polymers* **2022**, *14*, 4578. [CrossRef]
44. Kumari, S.; Yadav, B.S.; Yadav, R. Morphological and thermo-mechanical characterization of sweet potato starch based nanocomposites reinforced with barley starch nanoparticles. *J. Food Sci. Technol.* **2022**, *59*, 4924–4934. [CrossRef]
45. Ginzburg, V.V. Influence of nanoparticles on miscibility of polymer blends. A simple theory. *Macromolecules* **2005**, *38*, 2362–2367. [CrossRef]
46. Dimonie, D.; Radovici, C.; Pop, S.; Socoteanu, R.; Petre, C.; Fierascu, R.; Fierascu, I.; Zgarian, R.; Marius, P.; Coserea, R. Approaches Considering a Better Incorporation of Multilayered Silicate into a Polymeric Matrix Designed for Bio-Nano-Materials Obtaining. *Nonlinear Opt. Quantum Opt.-Concepts Mod. Opt.* **2012**, *44*, 137.
47. Xie, W.; Gao, Z.; Pan, W.-P.; Hunter, D.; Singh, A.; Vaia, R. Thermal degradation chemistry of alkyl quaternary ammonium montmorillonite. *Chem. Mater.* **2001**, *13*, 2979–2990. [CrossRef]
48. Chrissafis, K.; Bikiaris, D. Can nanoparticles really enhance thermal stability of polymers? Part I: An overview on thermal decomposition of addition polymers. *Thermochim. Acta* **2011**, *523*, 1–24. [CrossRef]
49. Liu, W.-C.; Halley, P.J.; Gilbert, R.G. Mechanism of degradation of starch, a highly branched polymer, during extrusion. *Macromolecules* **2010**, *43*, 2855–2864. [CrossRef]
50. Greenwood, C.T. The thermal degradation of starch. *Adv. Carbohydr. Chem.* **1967**, *22*, 483–515.
51. Dimonie, D.; Dragne, M.; Trica, B.; Nicolae, C.-A.; Raduly, M.; Doncea, S.; Ladaniuc, M.; Mustatea, A.; Miu, F.; Soare, L.; et al. New Biodegradable Materials for Re-Thought Packaging from Pre-Consumer Wastes by Controlling the Storage Time as Method to Increase the Mechanical Recycling Efficiency. *Materials* **2023**, *16*, 1503. [CrossRef]
52. Mohsin, M.; Hossin, A.; Haik, Y. Thermal and mechanical properties of poly (vinyl alcohol) plasticized with glycerol. *J. Appl. Polym. Sci.* **2011**, *122*, 3102–3109. [CrossRef]

53. Peng, Z.; Kong, L.X. A thermal degradation mechanism of polyvinyl alcohol/silica nanocomposites. *Polym. Degrad. Stab.* **2007**, *92*, 1061–1071. [CrossRef]
54. Tsuchiya, Y.; Sumi, K. Thermal decomposition products of poly (vinyl alcohol). *J. Polym. Sci. Part A-1 Polym. Chem.* **1969**, *7*, 3151–3158. [CrossRef]
55. Senkevich, S.I.; Druzhinina, T.V.; Kharchenko, I.M.; Kryazhev, Y.G. Thermal transformations of polyvinyl alcohol as a source for the preparation of carbon materials. *Solid Fuel Chem.* **2007**, *41*, 45–51. [CrossRef]
56. Holland, B.J.; Hay, J.N. The thermal degradation of poly (vinyl alcohol). *Polymer* **2001**, *42*, 6775–6783. [CrossRef]
57. Tim, A.O. *Understanding Polymer Processing: Process and Governing Equations*; Carl Hanser Verlag GmbH Co KG: Munich, Germany, 2010.
58. Bashir, M.A. Use of dynamic mechanical analysis (DMA) for characterizing interfacial interactions in filled polymers. *Solids* **2021**, *2*, 108–120. [CrossRef]
59. Westhoff, R.P.; Kwolek, W.F.; Otey, F.H. Starch-Polyvinyl Alcohol Films–Effect of Various Plasticizers. *Starch-Stärke* **1979**, *31*, 163–165. [CrossRef]
60. Javed, A.; Ullsten, H.; Järnström, L.; Ernstsson, M. Study of starch and starch-PVOH blends and effects of plasticizers on mechanical and barrier properties of coated paperboard. *Nord. Pulp Pap. Res. J.* **2016**, *31*, 499–510. [CrossRef]
61. Mohamed, R.; Mutalib, N.W.A.; Norizan, M.N.; Hirzin, R.S.N.; Isa, S.A.M. Effect of different plasticizers on tensile properties of PVA/sago starch system before and after weathering exposure. *AIP Conf. Proc.* **2018**, *1985*, 030005.
62. Aydın, A.A.; Ilberg, V. Effect of different polyol-based plasticizers on thermal properties of polyvinyl alcohol: Starch blends. *Carbohydr. Polym.* **2016**, *136*, 441–448. [CrossRef]
63. Michels, L.; Da Fonseca, C.L.S.; Méheust, Y.; Altoe, M.A.S.; Dos Santos, E.C.; Grassi, G.; Droppa Jr, R.; Knudsen, K.D.; Cavalcanti, L.P.; Hunvik, K.W.B. The Impact of Thermal History on Water Adsorption in a Synthetic Nanolayered Silicate with Intercalated Li^+ or Na^+. *J. Phys. Chem. C* **2020**, *124*, 24690–24703. [CrossRef]
64. Newman, A.C.D. The interaction of water with clay mineral surfaces. *Monogr. Mineral. Soc.* **1987**, *6*, 237–274.
65. Amorim, C.L.G.; Lopes, R.T.; Barroso, R.C.; Queiroz, J.C.; Alves, D.B.; Perez, C.A.; Schelin, H.R. Effect of clay–water interactions on clay swelling by X-ray diffraction. *Nucl. Instrum. Methods Phys. Res. Sect. A Accel. Spectrometers Detect. Assoc. Equip.* **2007**, *580*, 768–770. [CrossRef]
66. Lin, Y.T.; Smith, N.J.; Banerjee, J.; Agnello, G.; Manley, R.G.; Walczak, W.J.; Kim, S.H. Water adsorption on silica and calcium-boroaluminosilicate glass surfaces—Thickness and hydrogen bonding of water layer. *J. Am. Ceram. Soc.* **2021**, *104*, 1568–1580. [CrossRef]